31st Annual International Conference of the IEEE EMBS
Minneapolis, Minnesota, USA, September 2-6, 2009

Multispectral Microscopy and Cell Segmentation for Analysis of Thyroid Fine Needle Aspiration Cytology Smears

Xuqing Wu, James Thigpen, and Shishir K. Shah, *Senior Member, IEEE*

Abstract— **This paper discusses the needs for automated tools to aid in the diagnosis of thyroid nodules based on analysis of fine needle aspiration cytology smears. While conventional practices rely on the analysis of grey scale or RGB color images, we present a multispectral microscopy system that uses thirty-one spectral bands for analysis. Discussed are methods and results for system calibration and cell delineation.**

I. Introduction

Thyroid nodule is one of many common cancers. Nodules are more common in women and increase in frequency with age and with decreasing iodine intake. It has been estimated that up to 20% of the world population [1, 2] and approximately 50% of 60-year-old persons [3] have palpable thyroid nodule or nodules. In the US, up to 7% of the adult population has a palpable thyroid nodule [4]. The clinical spectrum ranges from the incidental, asymptotic, small, solitary nodule, in which the exclusion of cancer is a major concern, to the large, partly intrathoracic nodule that causes pressure symptoms, for which treatment is warranted regardless of cause [2]. The most common cytologic diagnoses of thyroid nodules are colloid nodules, cysts, thyroiditis, follicular neoplasm, and thyroid carcinomas. Colloid nodules are the most common and do not have an increased risk of malignancy, therefore, the choice of management is conservative. Follicular neoplasm includes follicular adenoma and follicular carcinoma, which cannot be distinguished visually from each other based on cytology and the management remains controversial [2] [5] [3]. Thyroid carcinoma occurs in roughly 10% of all palpable nodules and the management is surgical removal [6].

Recent advances in clinical oncology have significantly increased the survival rate for most cancer patients. Early detection of the disease has been partly responsible for improved outcomes. Cytological and histological assessment has played an integral and important role in cancer diagnosis and prognosis. It is critical for the detection and characterization of excised tissue and cells from nodules and to identify its malignancy level. Among early screening methods, fine needle aspiration (FNA) has been widely accepted as a first-line screening test in patients with thyroid nodule. The major role of thyroid fine needle aspiration cytology (FNAC) is to distinguish thyroid nodules that require surgical removal due to higher risk of malignancy from those benign lesions that can be managed conservatively. According to guidelines from American Association of Clinical Endocrinologists, fine needle aspiration (FNA) is believed to be the most effective method available for distinguishing between benign and malignant thyroid nodules [7]. Its utilization has increased in recent years partially because of increased diagnostic accuracy and wide availability of image-guided techniques, which allow smaller nodules to be detected and aspirated. In centers with experience in FNA, the use of this technique has been estimated to reduce the number of thyroidectomies by approximately 50%, to roughly double the surgical confirmation of carcinoma, and to reduce the overall cost of medical care by 25% [8], as compared with surgery performed on the basis of clinical findings alone.

In general, cytological diagnoses of thyroid disorders are divided into following categories: unsatisfactory/non-diagnostic, benign/negative for malignancy, indeterminate for malignancy, suspicious for malignancy, and positive for malignancy [9]. This is turn has exerted an increased impact on histological assessment in conjunction with early screening methods, moving it from an ancillary diagnostic tool to a stand-alone diagnostic procedure. FNAC is progressively replacing other methods such as radionucleotide scanning, because of more accurate diagnosis, expediency in obtaining treatment, overall cost of patientcare and smaller biopsy samples. As such there has been a concomitant increase in the demand for analysis tools for assessment of FNAC, with cell segmentation being a critical impediment to automated solutions. The cytodiagnosis of thyroid nodules by FNA is complex for the following reasons [10]:

- overlap of cytological patterns between neoplastic and non-neoplastic lesions.
- overlap of cytological features between neoplasms.
- coexistence of non-neoplastic and neoplastic processes and multiple malignancies in the same gland.

Currently, the "gold standard" for diagnosis of follicular adenoma and follicular carcinoma are histology. In many cases, the distinction between them can be difficult even on the postoperative histologic specimen [11]. Indeterminate or follicular lesions are thyroid lesions described as having cytologic evidence that may be compatible with malignancy but are not amenable to easy diagnosis. The recommendation

X. Wu and S. K. Shah are with the University of Houston, Dept. of Computer Science, Houston, TX 77204-3010, U.S.A. (corresponding author is S. K. Shah, phone: 713-743-3360; e-mail: shah@ cs.uh.edu).
J. Thigpen is with Unit of Work, LLC., Ellensburg, WA.

978-1-4244-3296-7/09/$25.00 ©2009 IEEE

for managing patients with nodules in this category is surgery. However, only about 30% of the cases are proved to be malignant on histology, remaining is benign which would be better managed by clinical follow up instead of surgery. Currently, there are no reliable methods to differentiate follicular adenoma from follicular carcinoma before surgery. We believe that spectral microscopy may provide additional information that can aid in improving the overall diagnostic accuracy [12]. Nonetheless, typical challenges of cell delineation remain to be addressed before an automated solution that can aid overall diagnostic effort can be developed.

In this paper, we present a multispectral microscopy system capable of acquiring spectral images under transmitted illumination and a watershed-based method for delineating cells. Several key steps have to be performed to automate this task, including system calibration, image acquisition, and cell segmentation. The remainder of the paper is organized as follows: section II presents the imaging system used to acquire spectral images and its relevance to FNAC smears analysis. The importance of calibration and the developed method is discussed. Section IV presents the segmentation approach used to delineate cells in the images along with obtained results on a dataset of images. Finally, conclusions appear in section V.

II. Multispectral Microscopy

Multispectral imaging combines two technologies that have independently evolved for the last several decades, namely spectroscopy and imaging. Systems that leverage the two technologies simultaneously have been used in the fields of astronomy [13], remote sensing [14], and chemical compound analysis [15] to identify the composition and characteristics of celestial, terrestrial, and atmospheric elements. In recent years, spectral imaging has also been used in biomedical applications such as spectral karyotyping [16], general cell visualization [17], cell trafficking of variously colored fluorescent proteins [18], and differentiation of pathologies [19]. Spectral imaging systems developed to facilitate various biomedical applications have typically been coupled with traditional microscopes to enable spectral microscopy. Spectral microscopes provide the combined benefits of spectroscopy and imaging microscopy, resulting in the ability to acquire spectral images of microscopic specimen.

More recently, multispectral microscopes capable of acquiring spectral images under transmitted illumination have also been used to digitize and analyze cell smears [12] [20]. Spectral imaging allows for the simultaneous measurement of spectral and spatial information of a sample such that the measurement of the spectral response at any pixel of a two-dimensional image is possible. Studies have shown that biological tissue exhibits unique spectra in transmission. By exploring the spectral differences in cellular pathology, many chemical and physical characteristics not revealed under traditional imaging systems can be realized and used to improve the analysis efforts.

We have assembled a multispectral microscopy system capable of acquiring spectral images under transmitted illumination. The system comprises of a standard light microscope coupled to a spectral dispersion component that separates the light into its spectral components. The microscope itself is coupled to a two-dimensional (2D) optical detector such as a CCD camera. In our case, we use a quarter-meter class, Czerny-Turner type monochromator from PTI (http://www.pti-nj.com) that provides a tunable light emission spectrum at 2nm resolution. We currently utilize a wavelength range from 400-700nm. The monochromator is connected to an Olympus (http://www.olympus.com) BX51 upright optical microscope such that the light output from the monochromator feeds into the transmitted light path of the microscope. An Olympus UPlanApo 40X NA 0.9 is used for imaging. The Photometrics SenSys™ CCD camera (http://www.roperscientific.com) having 768 x 512 pixels (9x9μm) at 8-bit digitization is used, which provides for high-resolution low light image acquisition. This camera is used for acquisition of spectral images.

To image each sample, the illumination from the monochromator is adjusted by achieving Kohler illumination for uniform excitation of the specimen. The condenser, aperture diaphragm, and the field stop are kept constant during measurements. To calibrate the variations due to illumination effects and varying quantum efficiency of CCD cameras at different wavelengths, we normalize the camera exposure for each wavelength while avoiding saturation. The underlying assumption is that the incident light should be uniform across all wavelengths. Since measurement of incident light is proportional to average background intensity, the problem of calibration is posed as computing exposures for each wavelength such that the resultant exposure values across the spectra generate uniform average background intensity. To achieve this objective, we pose the problem as one of equalizing the image Average Optical Density (AOD) across all the wavelength-exposure pairs. Wavelength-exposure pair images are the set of varying exposure images for each wavelength. A least square error solution is chosen to compute the final exposure values across the entire wavelength range [21].

The developed calibration algorithm has been integrated with our assembled automated microscope. Using a variety of commercial optical filters as standards, we have performed quantitative evaluation of the calibrated system. Manufacturers of optical filters quantify the stop- and pass-bands using well-tuned spectrophotometers and make the profiles available to end-users. We have compared the

measured spectral profile of several filters as obtained by our calibrated system. Figure 1 shows an overlay of manufacturer supplied and the measured profile for five different filters. In each of the cases, the profiles have over 98% correlation.

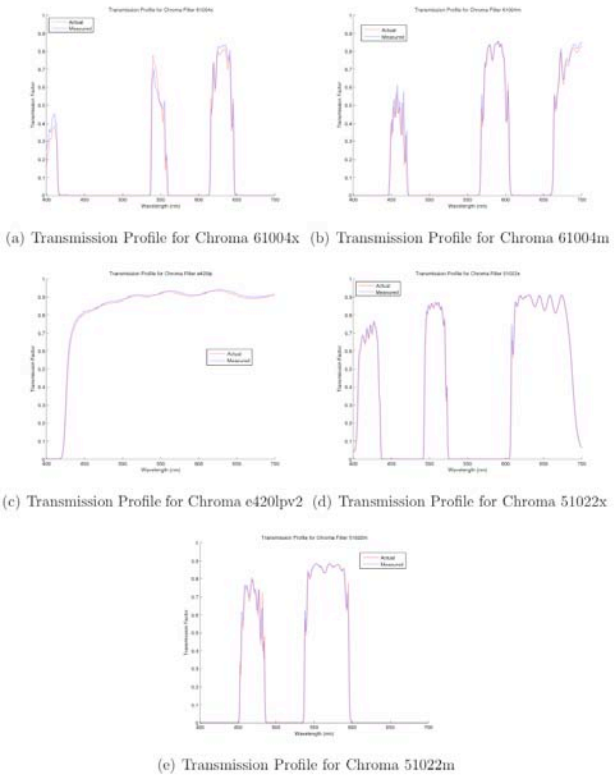

(a) Transmission Profile for Chroma 61004x (b) Transmission Profile for Chroma 61004m

(c) Transmission Profile for Chroma e420lpv2 (d) Transmission Profile for Chroma 51022x

(e) Transmission Profile for Chroma 51022m

Figure 1. Comparison of manufacturer supplied and measured spectral profile of five different filters using the calibrated spectral microscope.

Following calibration, automatic focusing is performed at the central wavelength of 550nm to minimize the chromatic aberration at all wavelengths. Spectral image set is acquired by stepping the monochromator from 400nm to 700nm illumination in 10nm increments, resulting in a total of 31 images for each field-of-view.

III. CELL SEGMENTATION

Watershed based method [22] has been preferred by many researchers and applied to the problem of cell image segmentation because of its ability to deal with touching and overlapped regions. In watersheds, a 2-D image is treated in three dimensions: two spatial coordinates versus gray levels. The gray level of each pixel represents the elevations of the watershed surface. Points at which water would be equally likely to fall into more than one minimum consist of the watershed lines. Points at which a drop of water would fall into a single minimum consist of catchment basin. Watershed lines separate catchment basin into non-overlapped regions [23]. It is a region growing method and groups of pixels called ``seeds'' are needed to initialize the growing process [24].

The initialization step is deemed as the most critical moment in a growing process [24]. Lezoray [25] suggested a supervised automatic clustering method, in which, each color plane is clustered independently by applying watershed operation on the gray-scale histogram. Each section in the cluster corresponds to a representative class of pixels in the image. The clustering information from different color planes is then blended together. However, spatial information is lost because of the use of the histogram. Touched cells are also clustered together in the supervised clustering process. To preserve the intensity variance information in the spatial domain, we apply an unsupervised clustering method to locate the ``seed'' for each region by using regional minima/maxima extraction.

Direct application of the watershed algorithm generally leads to over-segmentation problem due to noise and other local irregularities, such as the gradient [23]. We employ morphological self-dual reconstruction, which turns out to be extremely useful for image filtering and segmentation task [22]. Morphological self-dual reconstruction consists of reconstruction by geodesic dilation and erosion. This effectively reduces the intensity variance in a local area while preserving the intensity distribution information across the whole image. After applying morphological grayscale reconstruction to the image in each channel, the unsupervised clustering process is done by h-extrema extraction. In morphology, a regional minima M of an image f at elevation t is a connected component of pixels with the value t, such that every pixel in the neighborhood of M has a strictly higher value. To further suppress the irrelevant image features, we use h-minima transformation that will exclude all minima whose depth is lower or equal to a given threshold level h. This transformation is defined as the dual process of h-maxima extraction which is done by performing the reconstruction by dilation of f from $f-h$. The regional minima from each channel is fused to identify ``seeds'' for watershed initialization. In addition, edges in the image are enhanced to form constraints for the region growing process.

The above algorithm provides reasonable results for segmentation of cells in brightfield images. To enhance the algorithm for use with spectral images, we pre-process spectral image by leveraging absorption information calculated for each pixel across all spectral bands [21]. Specifically, we perform a hierarchical analysis based on band selection. The notion of band selection is based on selection or extraction of specific wavelength images from the spectral data cube that can maximize discriminative information for a specific task. We use Bhattacharyya distance as the discriminant measure to identify relevant spectral bands to be extracted for the purpose of maximizing separation of different cell types in the specimen [26]. Using the identified bands, a new image cube is generated and the developed enhanced watershed approach is used to segment

and delineate the cells.

In our preliminary findings, we imaged 20 thyroid FNAC smears stained with the Papanicolaou stain. Each smear was imaged at 40x magnification under both the multispectral imaging system and color imaging system. Images were manually analyzed to establish ground truth and a count of target cells in each image. Segmentation using multispectral absorption image excludes almost all the blood cells while segmentation using color image has difficulties in separating blood cells from target cells. For the entire dataset, the detection accuracy of the method applied to the absorption image is found to be 95.19% with a false positive rate of 2.12%. Accuracy of target cell segmentation increases less than one percentage compared to segmentation using the color image. However, 25.26% decrease in the false positive rate is achieved using the proposed method on the absorption image as compared to the color image. Figure 2(a) shows the results of cell delineation using the color image while figure 2(b) shows the results overlayed on a representative image from the spectral stack.

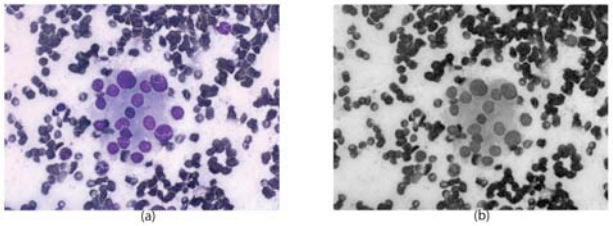

Figure 2. Result of applying watersheds segmentation on color image (a) and the corresponding spectral image (b).

IV. Conclusions

We have presented a multispectral imaging system and associated algorithms for calibration and cell segmentation for application in automated analysis of thyroid fine needle aspiration cytology smears. The automated system uses a standard optical microscope coupled with a monochromator to acquire spectral images under transmitted illumination. An algorithm for system calibration is presented which is necessary to correct for various interferences that occur during the imaging process that can affect the ability to quantify the images and compute true spectral profiles of cells of interest. An algorithm for automated cell segmentation using the spectral image stack is also presented. Results of segmentation are compared against those obtained by the use watershed-based cell segmentation on color images.

References

[1] L. Hegedus, "The thyroid nodule," *New Eng J Med.,* vol. 351, pp. 1764-1771, 2004.

[2] L. Hegedus, S. J. Bonnema, and F. N. Bennedbaek, "Management of simple nodular goiter: current status and future perspective," *Endocr Rev.,* vol. 24, pp. 102-132, 2003.

[3] F. N. Bennedbaek, H. Perrild, and L. Hegedus, "Diagnosis and treatment of solitary thyroid nodule: results of a North American survey," *J Clin Endocrinol Metab.,* vol. 85, pp. 2493-2498, 2000.

[4] P. A. Singer, D. S. Cooper, and G. H. D. et al., "Treatment guidelines for patients with thyroid nodules and well differentiated thyroid cancer," *Arch Intern Med.,* vol. 156, pp. 2165-2172, 1996.

[5] F. N. Bennedbaek, H. Perrild, and L. Hegedus, "Diagnosis and treatment of solitary thyroid nodule: results of a European survey," *Clin Endocrinol (Oxf).* vol. 50, pp. 357-363, 1999.

[6] E. L. Mazzaferi, "Management of a solitary thyroid nodule," *N Engl J Med.,* vol. 328, pp. 553-559, 1993.

[7] J. A. Feldman, " Dynamic Connections in Neural Networks," *Biological Cybernetics,* vol. 46, pp. 27-39, 1982.

[8] E. L. Mazzaferi, "Thyroid cancer in thyroid nodules: finding a needle in the haystack," *Am J Med.,* vol. 93, pp. 359-362, 1992.

[9] Society of Cytopathology, "Guidelines of the Papanicolaou Society of Cytopathology for the Examination of Fine-needle Aspitation Specimens from Thyroid Nodules," *Mod. Pathol.,* vol. 9, pp. 710-715, 1996.

[10] A. McCall, H. Jarosz, A. M. Lawrence, and E. Paloyan, "The Incidence of Thyroid Carcinoma in Solitary Cold Nodules and Multinodular Goiter," *Surgery,* vol. 100, pp. 1128-1132, 1986.

[11] J. Rosai, M. L. Carangiu, and R. A. DeLillis, "Atlas of tumor pathology," Washington, 1990, pp. 21-47.

[12] S. Shah, M. R. Schwartz, D. R. Mody, M. Scheiber-Pacht, and M. Amrikachi, "The Role of Multispectral Microscopy in Differentiating Benign and Malignant Thyroid Nodules: A Pilot Study of 24 Cases," in *Proceedings of the Annual Meeting of the United States and Canadian Academy of Pathology*, 2008.

[13] E. Kim, Y. Choi, H. S. Yang, M. Kang, S. Jeong, S. Yang, E. D. Kim, J. H. Lee, A. A. Rasheed, H. M. Nasir, and M. R. Rosdi, "A high-resolution multi-spectral imaging system for small satellites," *Acta Astronautica,* vol. 52(9), pp. 813-818, 2003.

[14] J. Kerekes and J. Baum, "Spectral imaging system analytical model for subpixel object detection," *IEEE Transactions on Geoscience and Remote Sensing,* vol. 40(5), pp. 1088-1101, 2002.

[15] A. Kulcke, C. Gurschler, G. Spock, R. Leitner, and M. Kraft, "On-line classification of synthetic polymers using near infrared spectral imaging," *Journal of near infrared spectroscopy,* vol. 11(1), pp. 71-81, 2003.

[16] S. Tsunoda et. al. , "Novel spectral imaging system combined with confocal laser microscopy for FISH analysis of interphase nuclei," *Cytometry,* p. 139, 2002.

[17] D. Maiti, S. Sennoune, and R. Martinez-Zaguilan, "Proton gradients in human breast cancer cells determined by confocal, multiphoton, and spectral imaging microscopy," *FASEB Journal,* vol. 17(4), p. A467, 2003.

[18] T. Haraguchi et. al. , "Spectral imaging fluorescence spectroscopy," *Genes to Cells,* vol. 7(9), pp. 881-887, 2002.

[19] K. Roy, I. Bottrill, D. Ingrams, M. Pankratov, E. Rebeiz, P. Woo, S. Shapshay, S. Kabani, and R. Manoharan, "Diagnostic fluorescence spectroscopy of oral mucosa," *Proceedings of SPIE,* vol. 2395, pp. 135-142, 1995.

[20] C. Feng, C. Shuzhen, and Z. Libo, "New abnormal cervical cell detection method of multi-spectral pap smears," *Wuhan University Journal of Natural Sciences,* vol. 12, pp. 476-480, 2007.

[21] S. Shah, J. Thigpen, F. Merchant, and K. Castleman, "Photometric Calibration for Automated Multispectral Imaging of Biological Samples," *Proceedings of 1st Workshop on Microscopic Image Analysis with Applications in Biology (in conjunction with MICCAI, Copenhagen),* pp. 27-33, 2006.

[22] L. Vincent and P. Soille, "Watersheds in Digital Spaces: An Efficient Algorithm Based on Immersion Simulations," *IEEE Trans. Pattern Analysis and Machine Intelligence,* vol. 13, pp. 583-598, 1991.

[23] P. Soille, *Morphological Image Analysis, Principles and Applications*: Springer-Verlag, 1999.

[24] O. Lezoray and H. Cardot, "Cooperation of Color Pixel Classification Schemes and Color Watershed: a study for microscopic images," *IEEE Transaction on Imaging Processing,* vol. 11, pp. 783-789, 2002.

[25] O. Lezoray, "Supervised Automatic Histogram Clustering and Watershed Segmentation Application to Microscopic Medical Color Images," *Image Anal Stereol,* vol. 22, pp. 113-120, 2003.

[26] X. Wu and S. K. Shah, "Comparative Analysis of Cell Segmentation Using Absorption and Color Images in Fine Needle Aspiration Cytology," in *IEEE International Conference on Systems, Man, and Cybernetics*, 2008.